Journal of Applied Fluid Mechanics, Vol. 17, No. 10, pp. 2169-2180, 2024.
Available online at www.jafmonline.net, ISSN 1735-3572, EISSN 1735-3645.
https://doi.org/10.47176/jafm.17.10.2584

Experimental Investigation on Performance of an Arc Transverse Injection in a Supersonic Combustor Flow

B. Kathiravan[1†], S. Niranjan[2] and A. Sureshkumar[3]

[1] *Department of Aeronautical Engineering, Rajalakshmi Engineering College, Chennai, Tamilnadu, 602105, India.*
[2] *Department of Aerospace Engineering, Madras Institute of Technology, Chennai, Tamilnadu, 600044, India*
[3] *Department of Aeronautical Engineering, KCG College of Technology, Chennai, Tamilnadu, 600097, India*

†Corresponding Author Email: kathiravan.b@rajalakshmi.edu.in

ABSTRACT

The design of a supersonic combustor ramjet engine has gained significant attention for futuristic air-breathing engines. Achieving efficient fuel mixing and complete combustion within a short period poses a substantial challenge. This study has directed efforts towards improving mixing and minimizing total pressure losses across the supersonic combustor to enhance performance. Experiments were conducted to investigate the influence of fuel injection geometry in the supersonic combustor with an entry Mach number of 2. Two different fuel orifice geometries, inclined at 45°, were considered. The investigation covered four different momentum flux ratios: 0.8, 1.0, 1.2, and 1.4 respectively. Various measurements were conducted to observe flow phenomena inside the supersonic combustion, including wall static pressure measurement, Schlieren visualization, exit Mach number and total pressure loss measurement. Without injection cases exhibited weaker compression and expansion inside the combustor. During injection, the rise in wall pressure indicated that the bow shock formed in front of the arc injection was slightly weaker than that of the circular injection. The impinging bow shock on the opposite wall also exhibited higher strength, resulting in a static pressure rise. As a result, the lower total pressure ratio across the shock indicates a higher momentum exchange between the main flow and the orifice. Therefore, arc injection has proven more effective in exchanging momentum inside the supersonic combustor. Consequently, the Mach number at the exit of the combustor was higher for the arc injection.

Article History

Received January 13, 2024
Revised March 20, 2024
Accepted April 22, 2024
Available online July 31, 2024

Keywords:

Scramjet
Arc injection
Supersonic combustor
Cross flow
Horse vortices

1. INTRODUCTION

A scramjet, or supersonic-combustion ramjet, is an air-breathing engine in which the airflow remains supersonic throughout the engine. Scramjet-powered vehicles operate at supersonic and hypersonic speeds up to Mach 6 and are intended to be operational even at Mach 15. Mixing and flame-holding limitations in supersonic combustion have been intriguing focal points in research, making the design and operation of scramjets challenging. The high speeds of parallel or near-parallel shear flows result in insufficient time for the fuel and airstream to mix within milliseconds inside the combustor. Hence, a long combustor is required to complete the mixing process. However, this is not an ideal consideration for the weight and drag of supersonic aircraft; therefore, a shorter length must be considered. Over the past few decades, various methods have been adopted to improve the air-fuel mixture. Different mixing enhancement techniques, such as transverse fuel injection, including the use of pylons, struts, vortex generators, angular injector slots, and multiple injector slots arranged in different fashions, have been explored. Historically, various methods have been adopted to perform transverse injection of fuel into supersonic flow, some of which are discussed here.

Vishwakarma and Vaidyanathan (2016) attempted a transverse injection of olive oil seeding particles through a circular injector slot located behind pylons of different sizes at various injection pressures. The results show that the initial penetration height and the spread rate of the jet increase with an increase in pylon size. Ogawa (2006) numerically investigated the influence of injector orifice geometry on mixing performance in supersonic flow. The study reveals that the leading-edge configuration of injector slots plays a significant role in determining vortex patterns that enable mixing. It was also noticed that

NOMENCLATURE

J	momentum flux ratio	i	injection pressure
L	combustor length	w	wall pressure
P	static pressure	1	settling chamber pressure
P_0	total pressure	2	combustor exit
V	velocity of fluid	∞	mainstream
X	port location	ρ	density of fluid
a	ambient pressure		

injection angles at and below 45 degrees exhibited favorable mixing characteristics.

Anazadehsayed et al. (2017) performed a numerical simulation of multijet transverse injection of air and hydrogen through an array of circular slots. The injection of air downstream of the fuel shows better mixing in the supersonic crossflow field. A similar study by Hu et al. (2019) involved liquid injection accompanied by upstream gas injection. The results show that liquid jet penetration and total pressure recovery decreased monotonically as the spacing between the gas and liquid injector slots increased. Shekarian et al. (2014) investigated the numerical effect of incident shock waves on supersonic transverse injection. Downstream impinging of the incident shock wave improved flame holder capability and mixing rate between fuel and air. Ye et al. (2018) explored the impact of plate vibration on the mixing and combustion of transverse hydrogen injection into a supersonic stream. Plate vibration in supersonic flow caused oscillations in combustion performance, increasing momentum flux ratio and penetration depth. Randolph et al. (1994) studied the effect of a pulsed crossflow jet in a supersonic stream. Pulse injection increased penetration depth and jet spreading rate. The pulsing of the jet did not alter the momentum flux ratio.

Ben-Yakar et al. (2006) investigated normal/angular injection, forming a three-dimensional bow shock. The bow shock and under-expanded jet created an adverse pressure gradient, causing separation shock and a separation region. Increasing the area of the recirculation zone upstream of the injector orifice enhanced mixing and flame-holding properties. The studies also discussed the expansion of the injected jet downstream, forming a Prandtl Meyer expansion fan and barrel shock and terminating by a Mach disk as shown in (Fig. 1). To enhance mixing properties, it was suggested to displace the Mach disk downstream and vertically away from the injector orifice. Further downstream, the jet deforms into counter-rotating vortices undergoing stretching-tilting-tearing due to Kelvin Helmholtz's instability. This information provides insights into the complex interactions and mechanisms involved in supersonic transverse injection for combustion applications.

You et al. (2013) numerically studied the complex flow structure of transverse injection using Detached Eddy Simulation (DES) and Reynolds Averaged Navier Stokes (RANS) methods. The DES model better captures unsteady shock features, mixing patterns, and mixing efficiency than the RANS model. Mahesh (2012) also reported the crossflow physical behavior of incompressible and compressible jet injection. It was

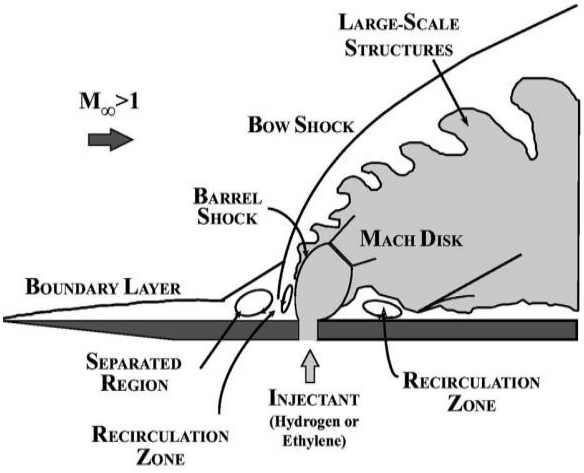

Fig. 1 Transverse injection into a supersonic flow (Ben-Yakar et al., 2006)

noted that vortex features change concerning orifice geometries.

Fric and Roshko (1994) observed that a tornado-like vortex structure is formed near the base of the jet where the boundary layer separates. Jet shear layer vortices and horseshoe vortices will also be present around the jet column exiting the orifice, which will help alter the mixing properties. To obtain and analyze a flow field due to transverse injection into a constant area duct, parameters such as momentum flux ratio, penetration height, bow shock standoff distance, mixing efficiency, jet to crossflow pressure and velocity ratios, jet stagnation to back pressure ratio, total pressure loss, and the spread area of jet particles can be controlled and observed. The momentum flux ratio is given by Eq.1:

$$J = \frac{\rho_i V_i^2}{\rho_\infty V_\infty^2} \tag{1}$$

Where ρ is the density, V is the velocity, J denotes the jet momentum flux ratio, and i and ∞ denote the injection flow and the mainstream of the combustor. The momentum flux ratio is an important parameter determining the flow pattern around the injector orifice and the shock strength (Schetz & Billig, 1966). It is also observed that for normal transverse injection, the penetration height is a function of 'J' and the longitudinal distance from the jet orifice only (Rothstein & Wantuck, 1992; Schindel & Abramovich, 2003). A higher rate of increase in jet spread area downstream indicates better mixing efficiency. Gutmark et al. (1989) have stated that non-circular slots can achieve higher mixing efficiency. Timnat (1990) experimentally optimized the penetration height for various injection angles between 30° and 60°,

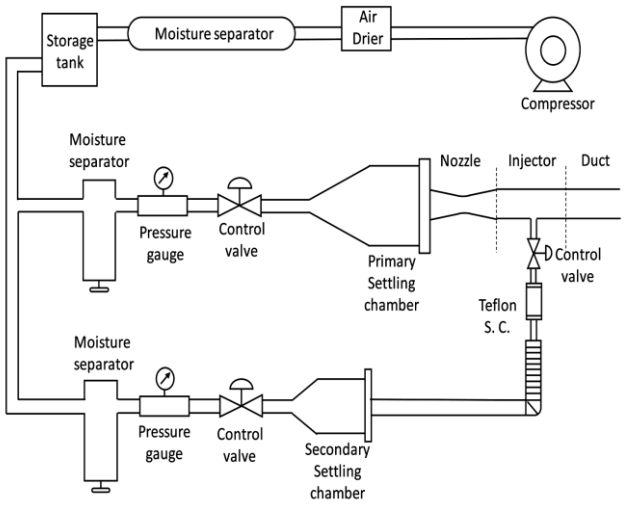

Fig. 2 Open Jet facilities with secondary injection setup

respectively. The results show that the injection angle of 45° had a higher penetration height.

Jeong et al. (2020) studied the effect of a non-axisymmetric cavity and non-circular cross-section with transverse injection in a supersonic combustor. The results revealed the advantages associated with angular injection in terms of diffusion and mixing characteristics, as well as the benefits of the cavity in terms of flame-holding capability. Athithan et al. (2021) conducted experimental and numerical investigations on the effects of placing dual ramps on opposite sides of the wall, ahead of a strut-type injector in a supersonic combustor. It was concluded that the configuration enhanced mixing characteristics by improving lateral fuel distribution and directing airflow towards the strut injector with reduced speeds due to the shocks formed by the presence of ramps. Relangi et al. (2021) proposed an axisymmetric cavity model for a circular cross-section supersonic combustor to inject fuel at various angles. It was observed that the cavity helped in flame holding and provided improvement in the mixing of fuel-air inside the combustor.

Zhao et al. (2022) attempted dual jet injection of water and hydrogen into a supersonic stream. The results showed that the dual injection method enhances the mixing rate. Han et al. (2023) numerically studied the cavity-based combustor model with boron powder fuel to estimate the combustion efficiency inside the supersonic combustor. The enhancement in mixing was observed when the particles are injected from the side wall of the cavity into the cavity rather than injecting upstream of the cavity. It was also noted that increasing the cavity depth resulted in higher combustion efficiency. Rajesh et al. (2023) performed experimental and numerical investigations to study the implications of dual cavity location in a strut-mounted scramjet combustor. It was found that the configuration increases combustion efficiency within a shorter combustor length, resulting in higher total pressure loss.

Most of the recent experimental and numerical investigations have focused on enhancing mixing through external configurations such as pylons, struts, and cavities. However, very few studies have been dedicated to enhancing mixing through fuel injection geometry and angular injection patterns inside the supersonic combustor. Hence, the present study proposes an investigation into one such injection geometric modification: arc transverse injection into the supersonic combustor duct. The study aims to compare the advantages of this method over conventional circular injection. Therefore, the present experimental investigation examines transverse injection at a 45° angle, considering two different orifice geometries: circular and arc injections. The flow features were characterized using wall pressure data and Schlieren images. The performance of these orifice geometries was evaluated based on total pressure loss and the exit Mach number of the combustor.

2. EXPERIMENTAL DETAILS

2.1 Open Jet Facility

The experiments were conducted in the open jet facility at the Propulsion Laboratory of Madras Institute of Technology, Chennai. Figure 2 illustrates the open jet facility and its various essential components arranged sequentially, including a compressor, air dryer, moisture separator, storage tank, pressure regulator, wide-angle diffuser, primary and secondary settling chambers, nozzles, and the test section as similar to Jabez Richards et al. (2023). Initially, atmospheric air is compressed using a two-stage 30hp reciprocating air compressor capable of providing a compressed air outlet with 90.3% efficiency. After compression, the air is supplied to the air dryer and the Moisture Separator. An air dryer typically uses a desiccant media to extract water vapor from the air, removing humidity and preventing the formation of new liquid. The dried air is stored in a high-pressure storage tank with a $1m^3$ volume capable of holding a working pressure of up to 14bar. The setup includes three separate moisture separators: one after the air dryer, one before the Primary Settling Chamber, and another before the Secondary Settling Chamber. These are connected after the Air Dryer and fitted with a pressure gauge to indicate the internal pressure. The facility has a pressure regulator before the secondary settling chamber, capable of measuring and regulating pressure up to 17bar. The test section is a single flange-mounted setup with top and bottom plates of the nozzle, injector section made of Mild Steel, and side walls made of acrylic sheets.

2.2 Supersonic Combustor Detail

A constant-area supersonic combustor is designed to operate with an inlet Mach number of 2.0, and its overall length is 100mm. To obtain a supersonic flow inside the combustor, it is connected to a convergent divergent nozzle with the area ratio of 1.68, which is having throat area of $120\ mm^2$ and exit area around $204\ mm^2$ respectively. Both circular and arc jet injections are introduced into the bottom wall of the combustor. The circular injection has a diameter of about 3mm with an inclination angle of 45° from the horizontal. The arc

Table 1 Momentum flux ratios and their total injection pressures required

S.No	Momentum Flux Ratio J	Inlet Total Pressure of Mainstream P_0 (bar)	Injector Total Pressure P_{0i} (bar)
1	0.8	4	3.6
2	1.0	4	4.5
3	1.2	4	5.4
4	1.4	4	6.3

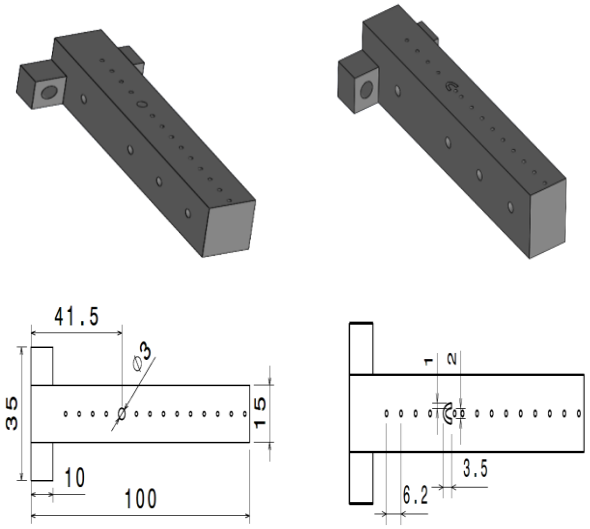

Fig. 3 Circular and Arc injection in the combustor model bottom plate and all dimension are in mm

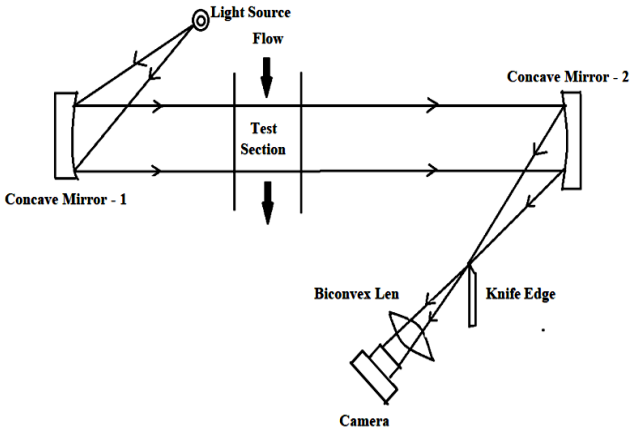

Fig. 4 Schlieren visualization setup

injection has semi-major and minor axes of 2.5mm and 1mm, respectively, with a thickness of a 1mm slot, and is set at the same inclination angle. However, the area of the injector mouth is kept constant for both cases. The injection geometries are shown in (Fig. 3).

2.3 Wall Pressure Measurements

Static pressure measurements of the wall are carried out by placing pressure ports that run through the thickness of the wall. These ports are spaced at different distances along the crossflow direction, as depicted in (Fig. 3). The inlet total pressure on the supersonic combustor is monitored based on the primary pressure gauge mounted with the pressure regulator as well as taping from the primary settling chamber. Exit total pressure is measured using a pitot tube placed at the exit of the combustor, ensuring blockage within permissible limits of 5%. The total pressure of the secondary injection is obtained by placing a port on the wall of the secondary settling chamber. This measurement is taken when the valve after the chamber is closed, creating a stagnant flow condition. All these ports are connected to a pressure scanner, which, in turn, is connected to a computer installed with Netscanner Unified Startup Software (NUSS). This software displays live mean gauge pressure readings. The 9116 Netscanner pneumatic intelligent pressure scanner, supplied by Measurement Specialties Inc., USA, consists of sixteen ports, and pressure measurements are taken with a sampling frequency of 500Hz and an accuracy of ±0.05% of full scale. The pressure ports at the base plate behind the injector slot run normally in the direction of crossflow, while those ahead of the injector slot are inclined at an angle of 45 degrees concerning the crossflow direction. Therefore, the former provides direct static pressure readings, while the latter is corrected for the inclination through calibration. The calibration results showed that the inclination accounted for 15% of the pressure measurements. The Table 1 shows the inlet conditions for both primary and secondary injection for different momentum flux.

2.4 Schlieren Visualization Technique

The supersonic flow field within a combustor duct is visualized using the Z-type Schlieren technique as shown in Fig. 4, employing a system comprising two concave mirrors, a light source, a knife edge, and a screen were similar to (Yazhini et al., 2021; Priyadharshini et al., 2022). A slit in the light source allows light to pass through, forming parallel rays upon reflection from the first concave mirror, which then traverse the test section. On the opposite side of the combustor duct model, another mirror collects and focuses the parallel rays to a point at the knife edge. The Schlieren technique operates based on the deflection of light beams crossing gradients in the index of reflection within a transparent medium. When encountering a density gradient in the test section, parallel rays of light are refracted, visualizing shock patterns during supersonic crossflow. Shock waves, characterized by thin regions of high pressure, temperature, and density gradients, cause the bending of light rays. These bent rays, obstructed by the knife edge, result in darkened lines in the recorded image where density gradients exist. The position of the knife edge is crucial for obtaining high-quality images of the flow field. Experiments are conducted in a dark environment to enhance the visibility of reflected rays on the screen, ensuring image quality. DSLR cameras are employed to record the shocks present throughout the experiment.

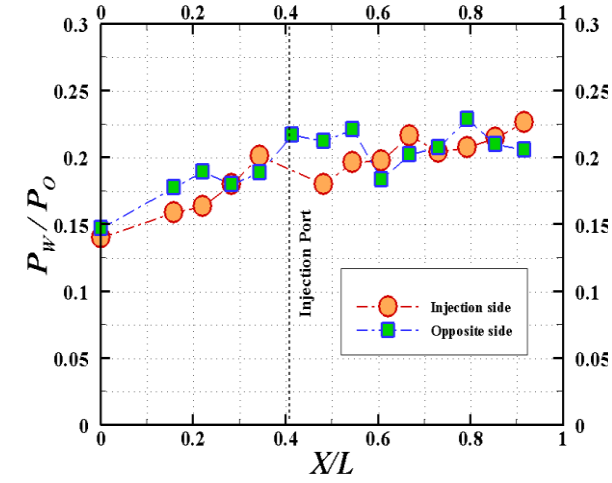

(a)

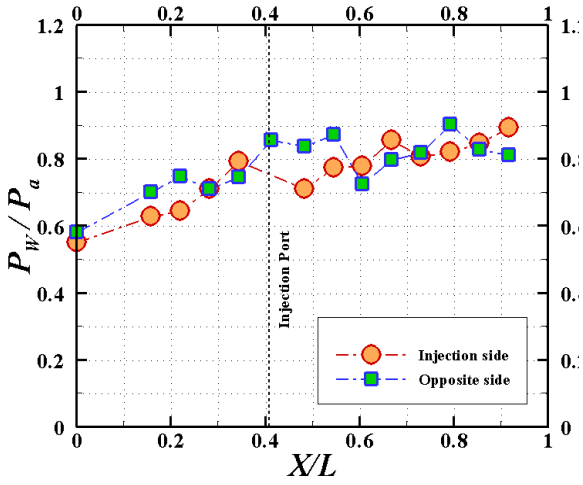

(b)

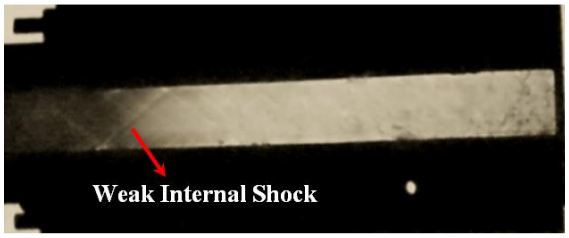

(c)

Fig. 5 Wall pressure data and shock image of circular injection (no-injection case)

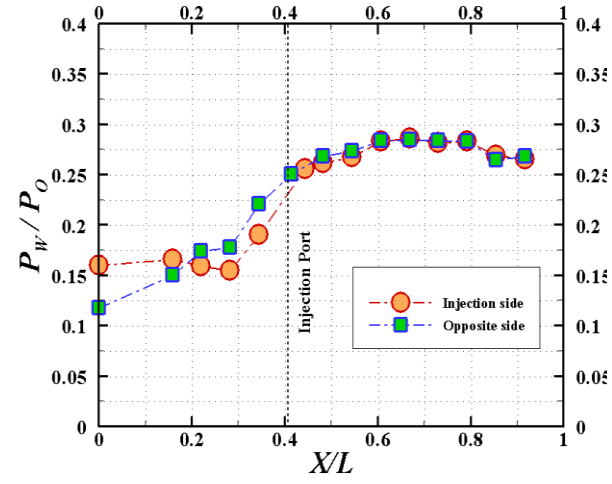

(a)

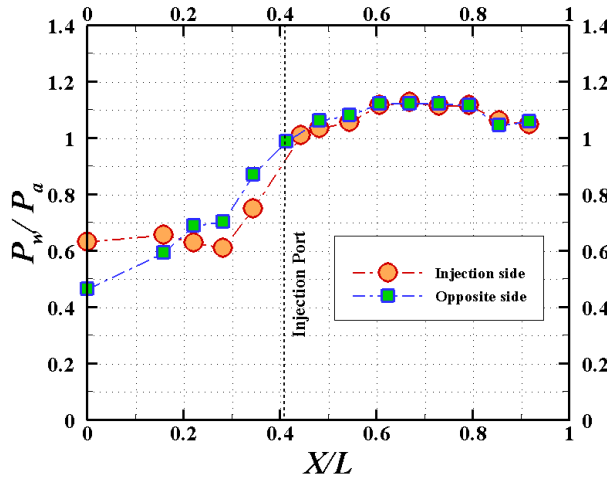

(b)

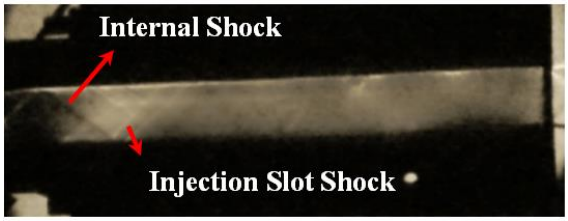

(c)

Fig. 6 Wall pressure data and shock image of Arc injection (no-injection case)

3. RESULTS AND DISCUSSION

Experiments were conducted for the four different values of 'J' factor for the inlet combustor pressure of 4 bar. In this section, wall static pressures, shock strength and shock structure were discussed for two different flows inside combustor as 'no-injection' and 'with injection' cases. The wall pressure measurements also well predict the flow characteristics of the internal flow Papamoschou et al. (2009). The total pressure at exit of the combustor was also estimated and compared between the two geometries.

3.1 Without Injection

Figures 5 and 6 show the wall pressure data and flow structure inside the supersonic combustion of circular and arc injection for no-injection cases. The wall pressure ports appear to be unsymmetrical between the injection and opposite sides of the combustor model due to presence of injection jet. The wall static pressure 'P_w' is non-dimensional, with settling chamber pressure 'P_0' and ambient pressure 'P_a,' respectively. These non-dimensional variables help predict the flow speed indirectly and flow separation inside the combustor. From Fig. 5a, it was observed that the flow initially enters with the pressure ratio varying between 0.14 and 0.147 for the circular case, which approximates the Mach numbers of 1.94 and 1.91, respectively. In the case of arc injection (Fig. 6a), the data shows values of 0.12 and 0.16, which approximate to Mach numbers of 2.03 and 1.87, respectively. This small variation in the pressure ratio may be due to variations in the entry geometries between the models. In the circular injection combustor, the wall

pressure ratio starts increasing from entry to exit with small fluctuations, indicating that the flow starts decelerating due to formation of weaker compression waves and accelerated due to expansion waves inside the combustor. The overall trend shows that pressure rise would be accounted for by Fanno flow occurring inside the duct. A similar trend was found in the arc geometry, but a sudden pressure rise is observed ahead of the fuel injection due to the presence of arc pattern holes generates weaker compression wave. On the other hand, the wall pressure variation without injection in the circular slotted duct shows an unsymmetrical shock pattern in the wall pressure data between the injection and the opposite side. In the middle section, pressure drop at some ports may occur due to expansion, and pressure rise might occur due to the impinging of weaker shocks. This was similar to the propagation of shock expansion in an isolator, as observed in the Schlieren image of (Fig. 5c).

In the case of arc injection, the pressure remains nearly constant at the entry of the combustor and starts to rise due to the shock wave generated near the injector hole. On the other hand, the flow continuously decelerates from entry, causing a pressure rise that eventually reaches equilibrium with the ambient pressure. Figure 6c shows a shock wave running from the bottom to the top wall inside the combustor, confirming this behavior. In the circular combustor, the ratio of P_w/P_a inside the combustor lies between 0.6 and 0.9 in (Fig 5b), indicates no wall separation based on the Summerfield criterion of P_w/P_a, which is approximately 0.35 - 0.40, respectively (Frey & Hagemann, 2000). However, in the case of arc injection in (Fig. 6b), the ratio crosses the value of P_w/P_a = 1.0 due to the higher strength of the shock wave inside the combustor.

3.2 With Injection

In this section, the comparison of circular and arc injection for various 'J' values is examined. Figure 7 shows the wall pressure measurements made between the injection and opposite side of the circular and arc injection at J = 0.0. From Fig.7a, it was observed that the arc slot might lead to the formation of a weaker shock, causing a tendency for the wall pressure to rise, as also observed in the schlieren image shown in (Fig.6c). A similar observation was made on the opposite wall, where the pressure rise starts gradually from the initial shock formed near the combustor entry. But, the circular combustor shows only small pressure fluctuations due to shock expansion wave interacts inside the combustor on either sides.

Figure 8 illustrates the wall pressure measurements data sets at J=0.8 for both circular and arc injection. In Fig. 8a it was observed that there is a sudden pressure peak inside the combustor, attributed to the formation of a bow shock and separation on the wall due to the pressure arising ahead of the slots during injection in both geometries. However, the peak pressure and shock location slightly differ between the geometries. In the case of arc injection, the peak pressure on the injection side is slightly higher, and the location of the shock is slightly downstream of the flow. The shockwave is slower to reach the injection port in the case of arc injection compared to circular injection. The flow starts to separate from the

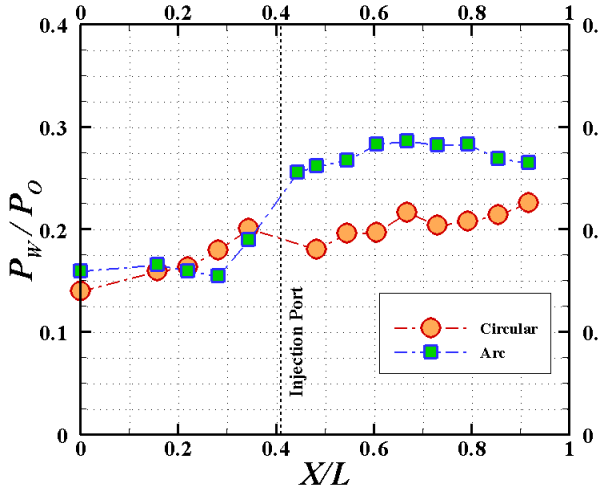

(a) Injection side wall pressure at J = 0.0

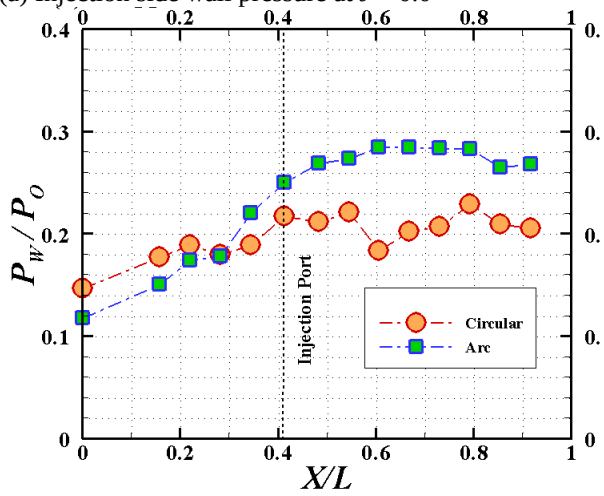

(b) Opposite side wall pressure at J = 0.0

Fig. 7 Wall pressure measurement of Circular and Arc injection at J = 0.0

circular injection a little ahead of the injection port, whereas in the case of the arc, separation starts somewhat downstream of the port. This is due to the wider spreading of the port in the case of arc injection.

The opposite wall of the circular injection also experiences a peak pressure behind the injection point. However, in the case of arc injection, the wall opposite the injection does not show such a peak. This indicates that the shock wave forming on the circular injection has higher penetration due to less dissipation of flow in the lateral direction, similar to its counterpart. The evolution of the jet inside the duct may have mild effects on the wall pressures downstream of the slot location. The jet evolves into a counter-rotating vortex pair surrounded by a varying momentum fluid interaction layer undergoing Kelvin-Helmholtz instability. These vortices may tend to reduce the wall static pressure. In the ports behind the slot location, the variation of wall static pressure with J is different for circular and arc injection ducts. In both ducts, there is a significant pressure drop in the port next to the slot location due to the recirculation zone behind the injection port. The rise in pressure in the consecutive port indicates flow reattachment. In the circular slotted duct,

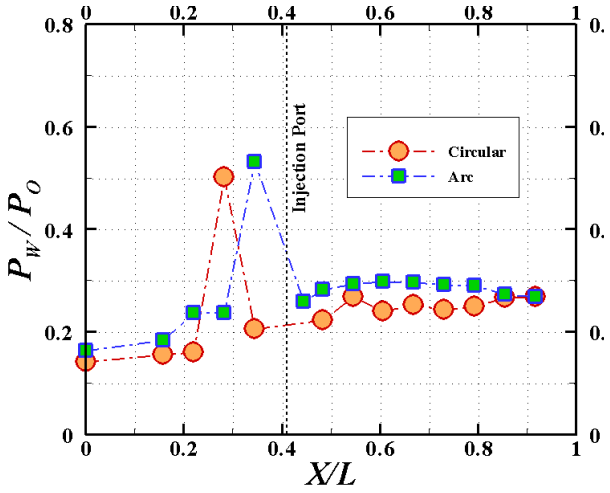

(a) Injection side wall pressure at J = 0.8

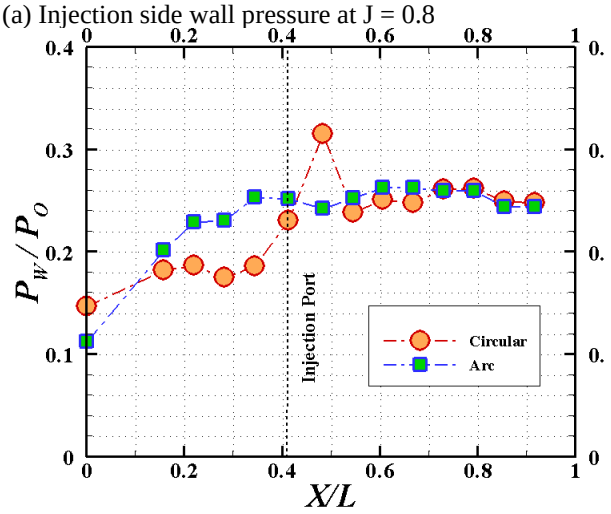

(b Opposite side wall pressure at J = 0.8

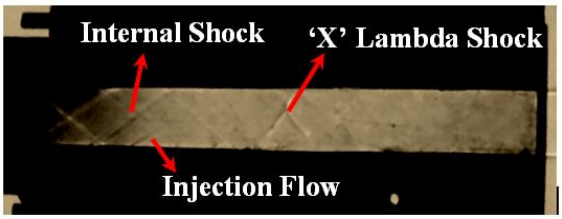

(c) Circular injection of J = 0.8

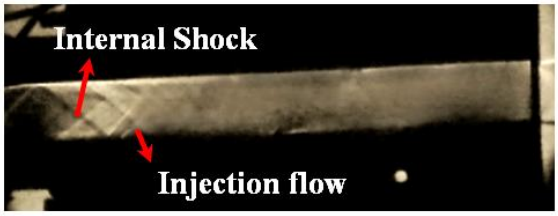

(d) Arc injection of J = 0.8

Fig. 8 Wall pressure measurement and shock images of Circular and Arc injection at J = 0.8

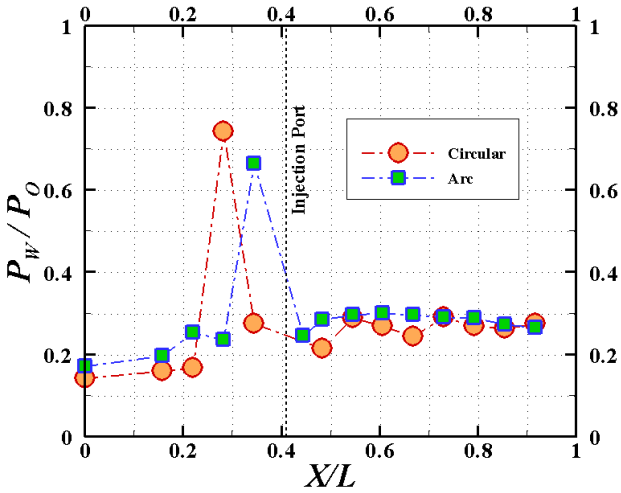

(a) Injection side wall pressure at J = 1.0

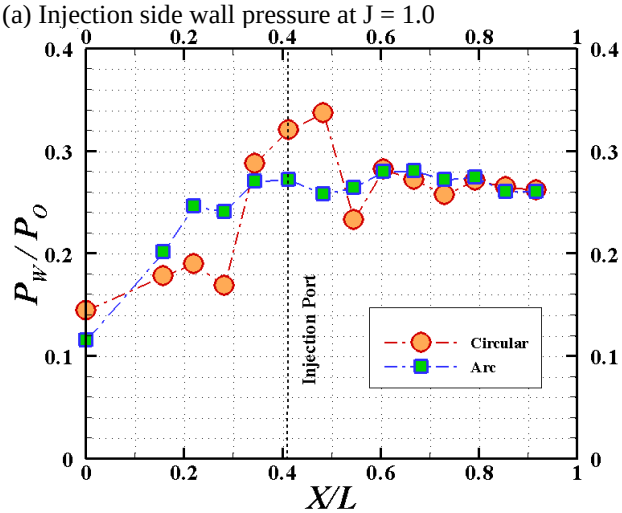

(b) Opposite side wall pressure at J = 1.0

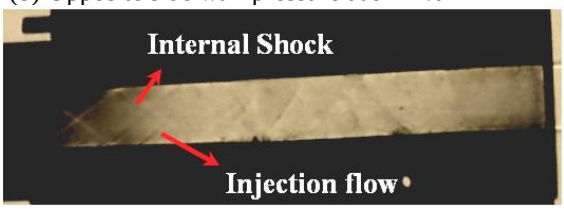

(c) Circular injection of J = 1.0

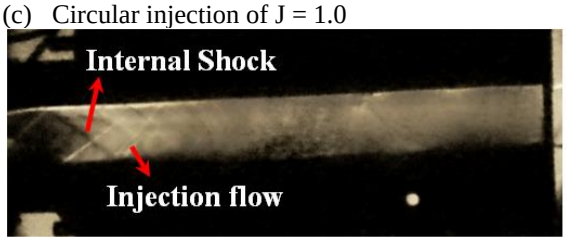

(d) Arc injection of J = 1.0

Fig. 9 Wall pressure measurement and shock images of Circular and Arc injection at J = 1.0

reattachment occurs between X/L=0.3 and X/L=0.4, whereas in the arc slotted duct, it has taken place a little downstream, between X/L=0.443 and X/L=0.5, respectively. This might be due to the extension of the arc injection slot.

As the J value increases from 0.8 to 1.0, the peak pressure increases with the momentum flux ratio (J value) for all other tested conditions, as observed in Figs 9 - 11.

Upon comparing these cases, the circular slotted configuration exhibits higher pressure peaks for increased J values. In contrast, in the arc-slotted configuration, the pressure peaks are smaller than in the circular-slotted configuration for all tested J values. The higher pressure peak in the circular slotted duct is attributed to the jet not spreading as fast and only penetrating. However, in the case of arc injection, the arc shape dissipates the jet momentum, causing faster mixing that may reduce the

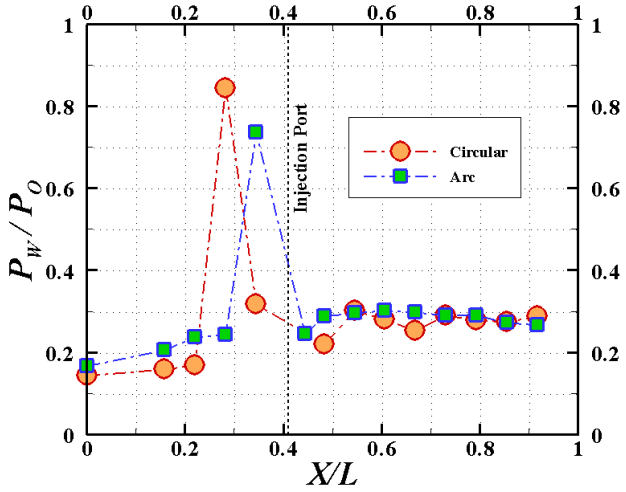

(a) Injection side wall pressure at J = 1.2

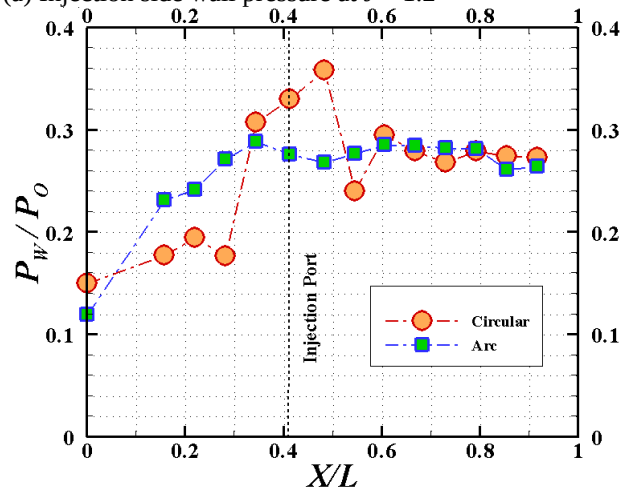

(b) Opposite side wall pressure at J = 1.2

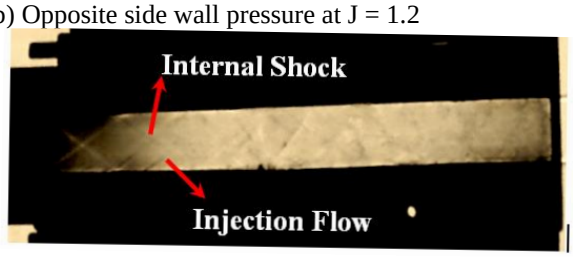

(c) Circular injection of J = 1.2

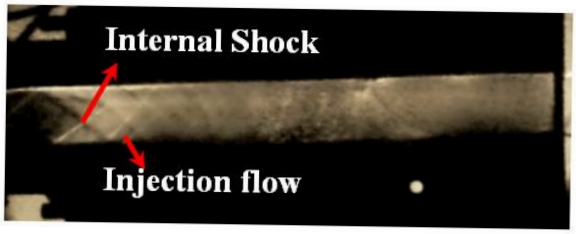

(d) Arc injection of J = 1.2

Fig. 10 Wall pressure measurement and shock images of Circular and Arc injection at J = 1.2

pressure peak. The flow field also indicates that the strength of the bow shock increases with an increase in the momentum flux ratio. Hence, total pressure loss is expected to increase with an increase in J values. The Schlieren images of injection in both ducts reveal an expansion fan facing downstream and inclined away from the downstream injection side wall. The inclination also increases with an increase in the J value, indicating that the initial penetration height increases when the momentum flux ratio is raised.

The location of the peak pressures in the circular slotted duct is ahead of that in the arc injection slotted duct. This denotes that the region between the separation shock and the leading edge of the slot is longer in the circular slotted duct. The injected jet entering into this region undergoes better mixing, and the region is also known for its flame-holding capability. The peak pressure in the arc-slotted duct may be due to the initial penetration of the jet occurring deeper in the arc-slotted duct than in the circular one. However, in other J values, the peak pressure arising in the circular jet is higher than in the arc jet. The jet spread rate is higher in the arc-slotted duct, leading to less pressure at the same location when J is increased. The opposite side wall pressures on both ducts confirm that the evolving jet is closer to the injection than the opposite side. However, on the opposite side, the circular jet shows a higher pressure rise due to shock impingement and wider pressure distribution from ahead of the impingement point. Similarly, the impingement of the shock on the opposite side occurs at the same point. However, the pressure data shows that the pressure peak on the opposite side also increases with the J value. The pressure trace along the arc injection was similar to that of no injection but slightly higher. This is because of the spreading nature of the elliptical injection, which also causes higher dissipation and formulates mixing with the main flow.

Upon comparing (Figs. 9 to 11), on the opposite side of circular and arc slotted ducts, a sudden rise in pressure can be observed in the circular slotted duct between 0.3 and 0.5 of X/L, respectively. This may be due to the bow shock hitting the opposite combustor wall. On the injection side, the shock originates around X/L of 0.2 and 0.3, respectively, for circular and arc injection. However, for J=0.8, the pressure rise starts at X/L=0.35 because the penetration height at lower J values is less, and the bow shock is not as steep as in the case of lower J values. Subsequently, there are sudden pressure drops at X/L= 0.55, possibly due to the flow expanding inside the combustor. In both ducts, in the ports before the injection location, pressure rises with an increase in J due to the upstream movement of weak shocks during injection.

The ports behind the slot location, the circular slotted duct, behave differently from the arc slotted duct. The wall pressures during injection are greater than those without injection in the case of the circular slotted duct. In contrast, the wall pressures during injection are less than without injection in the case of the arc duct. This can again be attributed to the higher spread rate in the arc-slotted duct. Graphs are plotted comparing the injection and opposite sides for each duct and each momentum flux ratio. These are in agreement with the corresponding Schlieren images. In all the plots, it is seen that injection side pressures are lower than opposite side pressures before the slot location. The vice versa occurs downstream of the slot location.

Figures 12 and 13 show the non-dimensional wall static pressure to ambient pressure to identify flow separation due to shock impingements through the Summerfield criterion (Frey & Hagemann, 2000), which

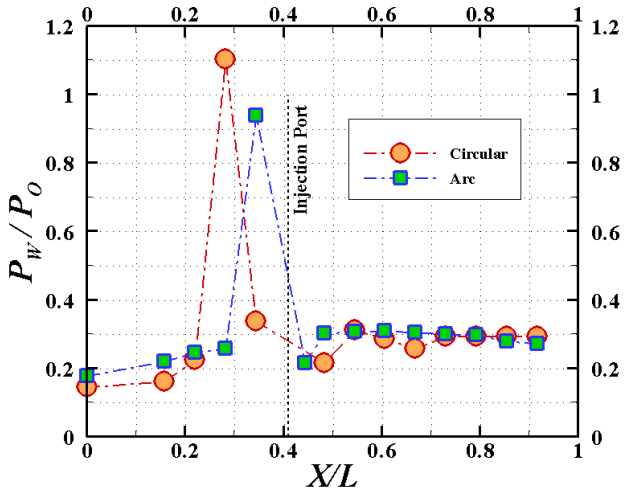

(a) Injection side wall pressure at J = 1.4

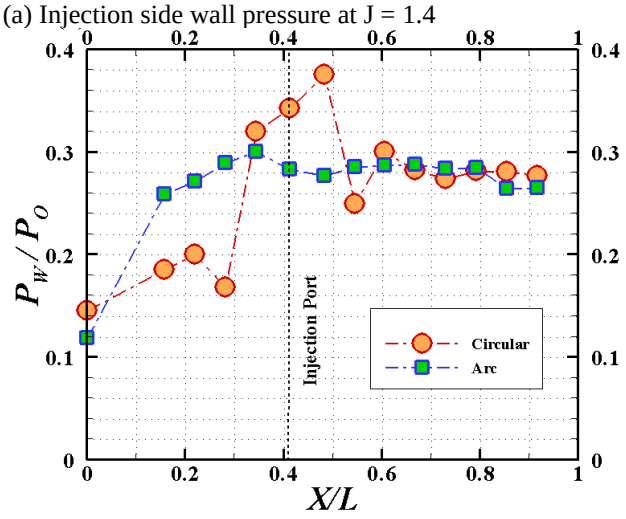

(b) Opposite side wall pressure at J = 1.4

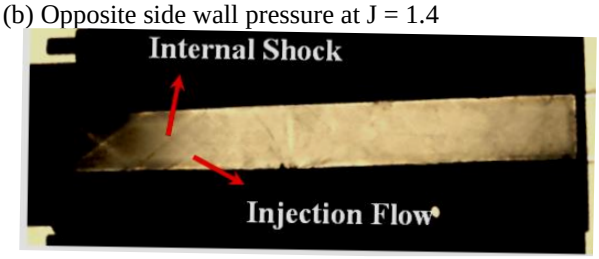

(c) Circular injection of J = 1.4

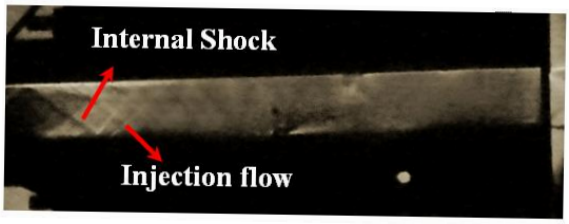

(d) Arc injection of J = 1.4

Fig. 11 Wall pressure measurement and shock images of Circular and Arc injection at J = 1.4

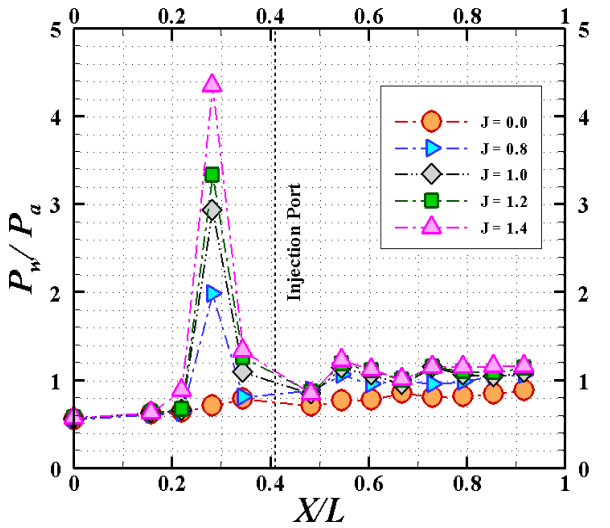

(a) Injection side wall pressure of Circular Injection

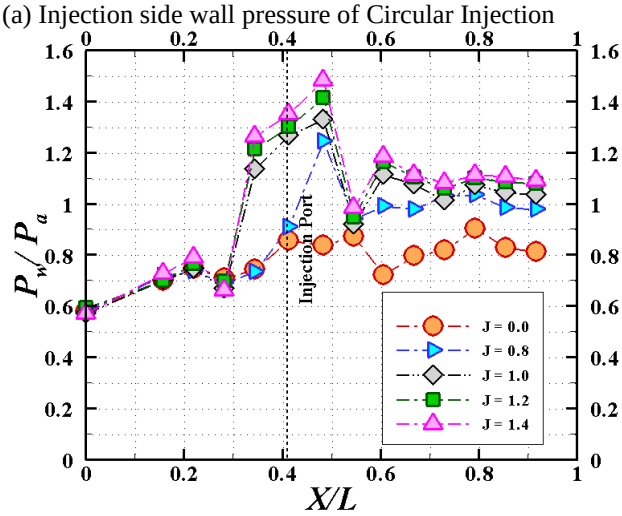

(b) Opposite side wall pressure of Circular Injection

Fig. 12 Non dimensional wall pressure for various J' value of circular injection.

was P_w approximated to 0.35 – 0.4 times of P_a, respectively. It was observed that there is a shock-induced separation inside both combustors even though the wall pressure was below the sub-atmospheric. In both cases of orifices, it was observed that the P_w/P_a in front of the injection port increases with increasing J value due to higher shock strength on the bottom plate. The wall pressure starts slightly earlier in the case of the arc geometry than the circular geometry. This is because of the boundary separation due to the formation of the shock wave more inclined towards the wall than a circular orifice. However, on the top side, the rise in pressure starts early in the case of arc jets compared to circular injection, but the parking pressure is observed for the circular case due to high penetration rather than spreading.

3.3 Exit Total Pressure and Mach Number

A pitot probe is used to measure the total pressure at the exit of the combustor for both circular and arc injection orifice geometries. The pitot probe is mounted at the center of the combustor exit to understand the momentum exchange between the main and orifice due to mixing in terms of total pressure ratios. A normal shock is formed in front of the probe when a pitot probe is inserted into a supersonic flow. Due to the formation of the shock wave, there is a pressure loss in front of the probe. The total pressure measured behind the shock is considered as P_{02}, which is non-dimensional concerning the main settling chamber pressure P_{01}, respectively.

Figure 14 shows the non-dimensional total pressure ratio for circular injection was higher than that for arc

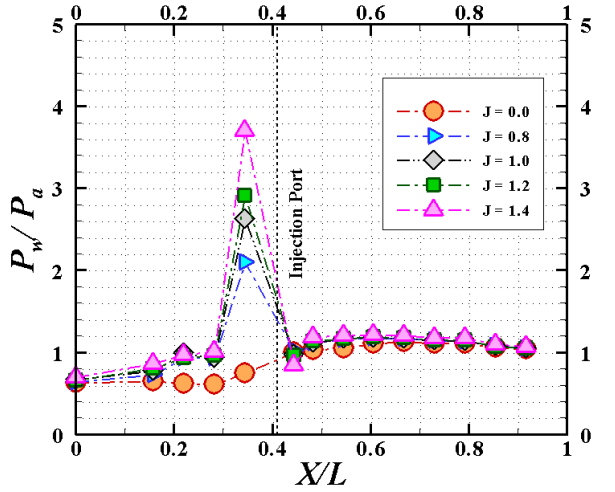

(a) Injection side wall pressure of Arc injection

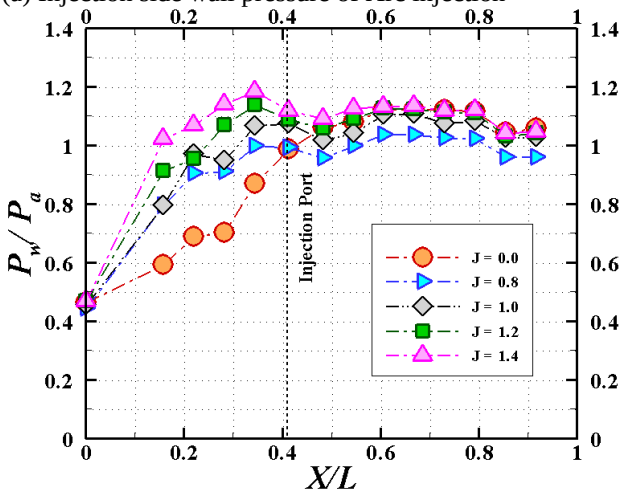

(b) Opposite side wall pressure of Arc Injection

Fig. 13 Non dimensional wall pressure for various J' value of arc injection

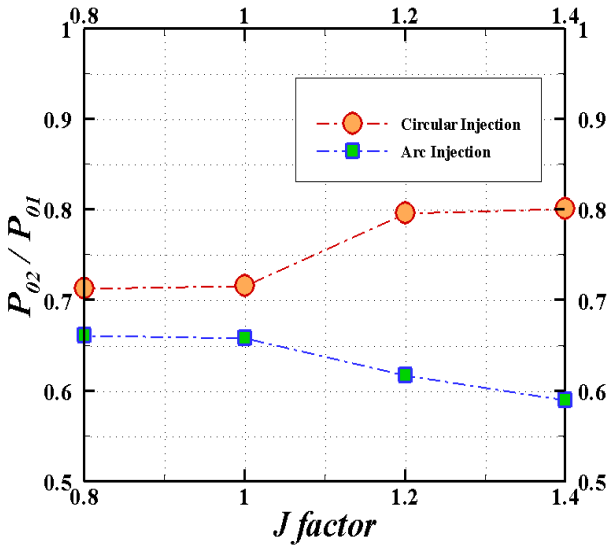

Fig. 14 Total pressure ratios at the combustor exit

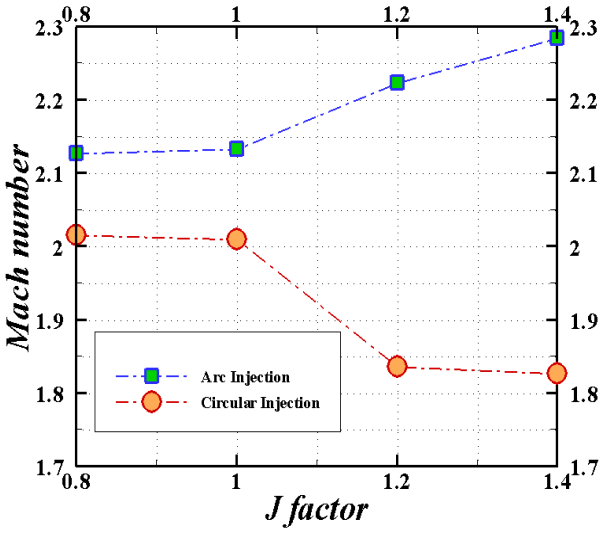

Fig. 15 Mach number at combustor exit

injection in all tested conditions. If the pressure ratio was higher, the strength of the shock wave was weaker. This means that the Mach number at the exit of the combustor was lower for the circular case compared to arc injection, which is calculated based on the normal shock, as shown in the Fig.15. The normal shock formed in front of the probe has a higher strength for a higher Mach number. This leads to a lower pitot pressure behind the shock. Hence, the Mach number of the arc injection was higher than that of the circular injection. This might be due to the high momentum available at the combustor exit for arc injection compared to circular injection. The higher momentum in arc injection confirms the mixing between the main flow and the orifice injection. As the momentum ratio increases, their mixing increases, causing a higher Mach number. This is also supported by the higher total pressure loss at the exit for higher J values. Hence, the arc injection orifice exchanges the momentum with the main flow more effectively than the circular orifice.

4. CONCLUSION

Experiments were conducted to predict the performance of circular and arc injection geometries at a transverse angle of 45° into a supersonic flow of Mach 2.0 at the entry of the combustor. The following conclusions were drawn from the experimental data:

- The momentum flux ratio 'J' significantly determined shock strength and initial penetration height. Circular injection exhibited higher penetration for J>1, while arc injection showed penetration for J<1.
- The total pressure ratio of arc injection was observed to have a lower value than circular injection, indicating normal shock strength. As the Mach number increased, the pressure ratio decreased.
- Arc injection enhanced the exit Mach number due to mixing between the main flow and injected mass at the end of the combustor.
- The shape of the injector slot significantly impacted total pressure loss, the separation region's size, and the reattachment point's location, and the jet spread area,

indirectly indicating penetration height at downstream locations.

- ❖ A faster spread rate is an indicator of better mixing efficiency. A circular slotted combustor is favored if the main concerns are initial penetration height and flame holding.
- ❖ The key factors considered for combustor design are minimum total pressure loss and mixing efficiency (faster spreading and mixing of the jet). In such cases, the suitable option for injector slot geometry would be a non-circular shape, such as arc injections.

ACKNOWLEDGEMENTS

Authors can acknowledge the contribution and help of those people or institutes that do not meet the authorship criteria. The responsibility of the information released within this section is completely on the corresponding author.

CONFLICT OF INTEREST

The authors declare that they have no known competing financial interests or personal relationships that could have appeared to influence the work reported in this paper.

AUTHORS CONTRIBUTION

Dr. B. Kathiravan: Conceptualization, Supervision, Writing – review & editing. **S. Niranjan:** Conceptualization; experimentation, Data curation, Writing-original draft. **Dr. A. Sureshkumar:** Formal analysis, Drafting, and supporting.

REFERENCES

Anazadehsayed, A., Barzegar Gerdroodbary, M., Amini, Y., & Moradi, R. (2017). Mixing augmentation of transverse hydrogen jet by injection of micro air jets in supersonic crossflow. *Acta Astronautica*, *137*(8), 403–414. https://doi.org/10.1016/j.actaastro.2017.05.007.

Athithan, A. A., Jeyakumar, S., Sivakumar, R. (2021, October). *The effect of ramp location in a strut based scramjet combustor under non reacting flow field.* IOP Conference Series: Materials Science and Engineering, 1128, International Conference on Applications in Computational Engineering and Sciences (IConACES 2020), Chennai, India. DOI 10.1088/1757-899X/1128/1/012006

Ben-Yakar, A., Mungal, M. G., & Hanson, R. K., (2006). Time evolution and mixing characteristics of hydrogen and ethylene transverse jets in supersonic crossflows. *Physics of Fluids*, *18*(2), 026101. https://doi.org/10.1063/1.2139684

Frey, M., & Hagemann, G. (2000). Restricted shock separation in rocket nozzles. *Journal of Propulsion and Power, 16* (3), 478-484. https://doi.org/10.2514/2.5593

Fric, T, F., & Roshko, D, A. (1994). Vortical structure in the wake of a transverse jet. *Journal of Fluid Mech, 279*, 1-47. https://doi.org/10.1017/S0022112094003800

Gutmark, E., Schadow, K. C., & Wilson, K, J. (1989). Noncircular jet dynamics in supersonic combustion. *Journal of Propulsion and Power*, *5*(5), 529–533. https://doi.org/10.2514/3.23186

Han, W., Hu, C., Li, J., Yang, J., Wei, R., Lei, R., & Li, C. (2024). Numerical investigation on the combustion characteristics of boron powder fuel under H_2/Air flame in a supersonic cavity-based combustor, *International Journal of Hydrogen Energy*, *53*, 343–352. https://doi.org/10.1016/j.ijhydene.2023.12.081

Hu, R., Li, Q., Li, C., & Li, C., (2019). Effects of an accompanied gas jet on transverse liquid injection in a supersonic crossflow. *Acta Astronautica*, *159*, 440–451. https://doi.org/10.1016/j.actaastro.2019.01.040

Jabez Richards, S. B., Thanigaiarasu, S., & Kaushik, M. (2023). Experimental study on the effect of tabs with asymmetric projections on the mixing characteristics of subsonic jets. *Journal of Applied Fluid Mechanics*, *16*(6), 1208–1217. https://doi.org/10.47176/jafm.16.06.1584

Jeong, E., O'Byrne, S., Jeung, I. S., & Houwing, A. F. P. (2020). The Effect of fuel injection location on supersonic hydrogen combustion in a cavity-based model scramjet combustor. *Energies*, *13*, 193, 1-16. https://doi.org/10.3390/en13010193

Mahesh, K. (2012). The interaction of jets with crossflow. *Annual Review of Fluid Mechanics*, *45*, 379-407. https://doi.org/10.1146/annurev-fluid-120710-101115

Ogawa, H. (2016). Effects of injection angle and pressure on mixing performance of fuel injection via various geometries for upstream-fuel-injected scramjets. *Acta Astronautica*, *128*(11), 485–498. https://doi.org/10.1016/j.actaastro.2016.08.008

Papamoschou, D., Zill, A., & Johnson, A. (2009). Supersonic flow separation in planar nozzles. *Shock Waves*, *19*(3), 171–183. https://doi.org/10.1007/s00193-008-0160-z

Priyadharshini, S., Muruganandam, T. M., & Kathiravan, B. (2022). Effect of flap deflection on performance of single expansion ramp nozzles at different pressure ratio. *Journal of Propulsion and Power*, *38* (6), 1025-1041. https://doi.org/10.2514/1.B38680

Rajesh, A. C., Jeyakumar, S., Jayaraman, K., Karaca, M., & Athithan, A. A. (2023). The implications of dual cavity location in a strut-mounted scramjet combustor, *International Communications in Heat and Mass Transfer*, *145*, 106855. https://doi.org/10.1016/j.icheatmasstransfer.2023.106855

Randolph, H., Chew, L., & Johari, H. (1994). Pulsed jets in supersonic crossflow. *Journal of Propulsion and*

Power, *10*(5), 746–748. https://doi.org/10.2514/3.23790

Relangi, N., Ingenito, A., & Jeyakumar, S. (2021). The implication of injection locations in an axisymmetric cavity-based scramjet combustor. *Energies*, *14*, 1-13. https://doi.org/10.3390/en14092626

Rothstein, A., & Wantuck, P. (1992, July). *A study of the normal injection of hydrogen into a heated supersonicflow using planar laser-induced fluorescence*. AIAA, SAE, ASME, and ASEE, 28th Joint Propulsion Conference and Exhibit, Nashville, TN, USA. https://doi.org/10.2514/6.1992-3423

Schetz, J. A., & Billig, F, S. (1966). Penetration of gaseous jets injected into a supersonic stream. *Journal of Spacecraft and Rockets*, *3*(11), 1658–1665. https://doi.org/10.2514/3.28721

Schindel, L., & Abramovich, G, N., (2003). *The theory of turbulent jets.* The MIT Press. https://doi.org/10.7551/mitpress/6781.001.0001

Shekarian, A. A., Tabejamaat, S., & Shoraka, Y. (2014). Effects of incident shock wave on mixing and flame holding of hydrogen in supersonic air flow. *International Journal of Hydrogen Energy*, *39*(19), 10284–10292. https://doi.org/10.1016/j.ijhydene.2014.04.154

Timnat, Y, M. (1990). Recent developments in ramjets, ducted rockets and scramjets. *Progress in Aerospace Sciences*, *27*(3), 201–235, https://doi.org/10.1016/0376-0421(90)90007-7

Vishwakarma, M., & Vaidyanathan, A. (2016). Experimental study of mixing enhancement using pylon in supersonic flow. *Acta Astronautica*, *118*, 21–32. https://doi.org/10.1016/j.actaastro.2015.09.011

Yazhini, V. I., Kathiravan, B., Muruganandan, T, M., & Jayaraman, K. (2021). Cowl length variation on performance characteristics of a single expansion ramp nozzle. *Journal of Propulsion and Power*, *37*(5), 780-791. https://doi.org/10.2514/1.B38217

Ye, K., Ye, Z., Li, C., & Wu, J., (2018). Numerical investigation on the mechanism of the effects of plate vibration on mixing and combustion of transverse hydrogen injection. *International Journal of Hydrogen Energy*, *43*, 22636–22648. https://doi.org/10.1016/j.ijhydene.2018.10.123

You, Y., Luedeke, H., & Hannemann, K., (2013). Injection and mixing in a scramjet combustor: DES and RANS studies. *Proceedings of the Combustion Institute*, *34*(2), 2083–2092. https://doi.org/10.1016/j.proci.2012.10.001

Zhao, J., Lin, W., Yan, C., Zheng, Z., Tong, Y., & Nie, W. (2022). (2022). Mixing enhancement mechanism of combined H2-Water jets in supersonic crossflows in a combustor with an expanded section, *International Journal of Hydrogen Energy*, *47*, 10747 - 10761. https://doi.org/10.1016/j.ijhydene.2022.01.070.